

Using the “Switchable” Quality of Liquid Crystal Solvents To Mediate Segregation between Coil and Liquid Crystalline Polymers

Neal R. Scruggs and Julia A. Kornfield*

Division of Chemistry and Chemical Engineering, California Institute of Technology, Pasadena, California 91125

Jyotsana Lal

Intense Pulsed Neutron Source, Argonne National Laboratory, Argonne, Illinois 60439

Received November 11, 2005; Revised Manuscript Received April 5, 2006

ABSTRACT: The discontinuous change in solvent quality of a liquid crystal (LC) solvent, 5CB, at the nematic–isotropic phase transition produces abrupt changes in the phase behavior of solutions of coil and LC polymers and in the self-assembly of coil–LC block copolymers. Nematic 5CB is strongly selective for a side-group liquid crystal polymer (SGLCP), and isotropic 5CB is a good solvent for both SGLCP and a random coil (polystyrene, PS). In nematic 5CB, unfavorable LC–PS interactions drive phase separation in SGLCP–PS–LC ternary solutions and drive micellization of PS–SGLCP diblocks. In isotropic 5CB, rich phase behavior occurs in both ternary solutions and block copolymer solutions. Despite the fact that isotropic 5CB is a good solvent for both SGLCP and PS, segregation can occur due to the asymmetric solvent effect (i.e., the preference of the solvent for the SGLCP). In concentrated isotropic solutions, unfavorable SGLCP–PS interactions become dominant.

Introduction

Microphase separation in diblock copolymer melts is a well-understood phenomenon that allows access to a wide range of morphologies that find application in nanotechnologies, as reviewed by Park, Yoon, and Thomas.¹ The symmetry and length scale of the ordered state are controlled by selection of the chemical structure, connectivity, and relative lengths of the component blocks.² Binary thermodynamic interactions between the polymer blocks ultimately determine the block copolymer's nanostructure in the melt. In solution, thermodynamic interactions with a third component modulate the self-assembled structure: a fixed block copolymer at a fixed concentration can adopt various morphologies depending on the solvent.^{3–10} Block copolymers in selective solvents are used as rheology modifiers and drug delivery systems, for examples, and are also of fundamental interest because of the rich thermodynamics governing their self-assembly.

The choice of solvent heavily influences the equilibrium microstructure of AB diblock copolymer micelles.^{3,5–8} Partitioning of the solvent between the microdomains rich in block A and those rich in block B is referred to as the solvent's “selectivity” and is determined by thermodynamic interaction parameters between the solvent (S) and each polymer, χ_{AS} and χ_{BS} .^{11–15} In the limit of strong selectivity toward A ($\chi_{BS} \gg \chi_{AS}$), diblock copolymers form micelles with cores composed of B almost completely devoid of solvent. In contrast, a neutral, or nonselective, solvent partitions between core and corona. In the former case, dense-core micelles are formed having stronger intermicelle interaction potentials than the highly swollen, soft micelles afforded in the latter case.^{16,17}

When the solvent is a small-molecule thermotropic liquid crystal (LC), the phase behavior of a dissolved block copolymer is enriched by the discontinuous change in quality at the LC phase transitions. The simplest example is the transition from the nematic to the isotropic phase. The orientational order of the LC in the nematic phase presents a large entropic penalty

to solvation of a random coil polymer, but in the isotropic phase the solvent's spherical symmetry imposes no such solubility constraints.^{18,19} In contrast to a random coil polymer, a side-group liquid crystalline polymer (SGLCP) can undergo the change in orientational order with the LC solvent, making it soluble in both the nematic and isotropic phases. A coil–SGLCP block copolymer in a LC solvent can switch from being dissolved in a strongly selective solvent to being dissolved in a good solvent for both blocks when the first-order transition from the nematic to isotropic phase takes place. Such abrupt changes in solvent quality do not occur in non-LC solvents, and we term the phenomenon “switchable solvent quality”. We demonstrate that the jump in solvent quality indeed produces an abrupt change in the self-assembly of block copolymers, specifically a change in micelle structure of diblock coil–SGLCP in solution. We infer the driving force for block copolymer self-assembly from the phase behavior of ternary homopolymer solutions and further demonstrate that exceptional sensitivity to temperature and concentration allows the dominant driving force for block copolymer self-assembly to be modulated with small changes to these parameters.

Experimental Section

Materials. Polymer-analogous synthesis was used to make a SGLCP homopolymer and coil–SGLCP diblock copolymer. The pendant vinyl groups of a 1,2-polybutadiene homopolymer (65 kg/mol) or a poly[styrene-*block*-(1,2-butadiene)] (70 kg/mol PS, 97 kg/mol PB) diblock copolymer were functionalized with mesogenic side groups according to published methods²⁰ to yield HSiCB4 and ABSiCB4, respectively (Figure 1). The bulk polymers are nematic from room temperature up to an isotropization point of 60 °C for HSiCB4²⁰ and 51 °C for ABSiCB4.

Solutions of these polymers in the nematic LC 4-pentyl-4'-cyanobiphenyl (5CB) were prepared by dissolving the polymer and 5CB together in dichloromethane (DCM) and then evaporating the DCM under vacuum for at least 1 day.

Methods. a. Optical Microscopy of Homopolymers Dissolved in 5CB. Ternary mixtures of SGLCP homopolymer and polystyrene (PS) in 5CB were made by combining PS homopolymer (44 kg/mol GPC standard used as received from Aldrich) with HSiCB4

* Corresponding author: E-mail: jak@cheme.caltech.edu.

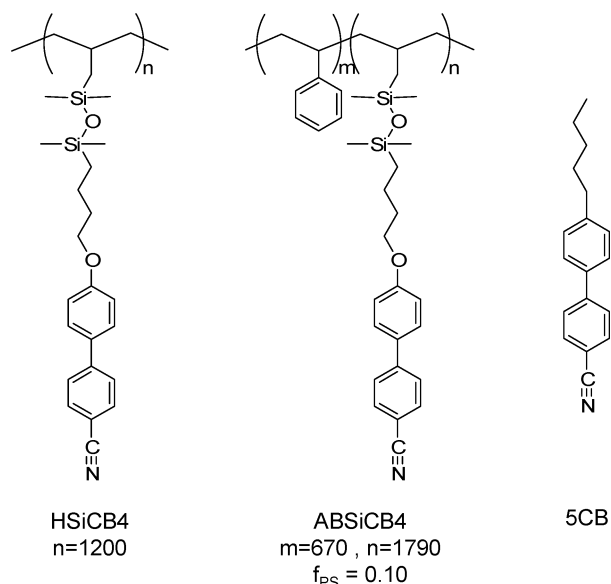


Figure 1. Chemical structure of the side-group liquid crystal homopolymer (HSiCB4), diblock copolymer (ABSiCB4), and the nematic liquid crystal solvent (5CB).

and 5CB in controlled quantities for a total mass of ~ 50 mg and then dissolving the three components together in 100 μL of tetrahydrofuran (THF). Samples were mixed for at least an hour to ensure complete dissolution of all three components. A small drop of the THF solution was placed in the shallow well of an indented microscope slide, and the THF was evaporated away at elevated temperature (~ 100 $^{\circ}\text{C}$). Slides were examined using a Zeiss optical microscope equipped with a Mettler FP82 hot stage and removable polarizers. Each sample was first heated from room temperature at a rate of 2 $^{\circ}\text{C}/\text{min}$ to observe the nematic-to-isotropic phase transition; viewed between crossed polarizers, the temperature at which the colorful, birefringent texture disappeared was recorded as the isotropization point (T_{NI}). Next, the polarizers were removed, and the sample was heated further until droplets characteristic of two-phase, isotropic/isotropic coexistence were no longer observed. Then, the sample was cooled at a rate of 10 $^{\circ}\text{C}/\text{min}$, and the temperature at which droplets reappeared was recorded as a nominal upper critical solution temperature (UCST). This measurement was repeated five times, examining a different area on the slide each time, and the results were averaged. To set a bound on the subcooling required for observable drops to form, several samples were raised to 5 $^{\circ}\text{C}$ above the nominal UCST. Consistently, a single phase formed over time. Therefore, the true UCST lies within 5 $^{\circ}\text{C}$ of the nominal one. Since the changes in UCST were very large, this uncertainty did not affect the conclusions of this study.

b. Rheometry of Diblocks Dissolved in 5CB. The frequency-dependent complex viscosity, $[\eta^*]$, under oscillatory shear was measured for 5CB and for 5, 10, and 20 wt % solutions of ABSiCB4 in 5CB using a TA Instruments ARES-RFS rheometer equipped with a 25 mm titanium cone and plate shear cell and a Peltier temperature controller. Data were collected at temperatures between 15 and 100 $^{\circ}\text{C}$, using 1 $^{\circ}\text{C}$ temperature increments near T_{NI} .

c. Small-Angle Neutron Scattering (SANS) of Diblocks Dissolved in 5CB. Diblock copolymer ABSiCB4 was dissolved in perdeuterated 5CB²¹ at concentrations of 2, 5, 10, and 20 wt % polymer and studied at two temperatures: in the nematic phase at 25 $^{\circ}\text{C}$ and in the isotropic phase at 37 $^{\circ}\text{C}$. The scattered intensity as a function of the scattering vector, $q = 4\pi/\lambda \sin \theta$, was recorded using the small-angle scattering instrument (SASI) at Argonne National Laboratory's Intense Pulsed Neutron Source (Argonne, IL). Measurements in the nematic phase were performed with LC director parallel to the neutron beam, allowing the two-dimensional scattering patterns to be azimuthally averaged. Uniform homeotropic alignment of the LC director was achieved by shearing the samples between glass plates; like triblock copolymer gels,²² the diblock

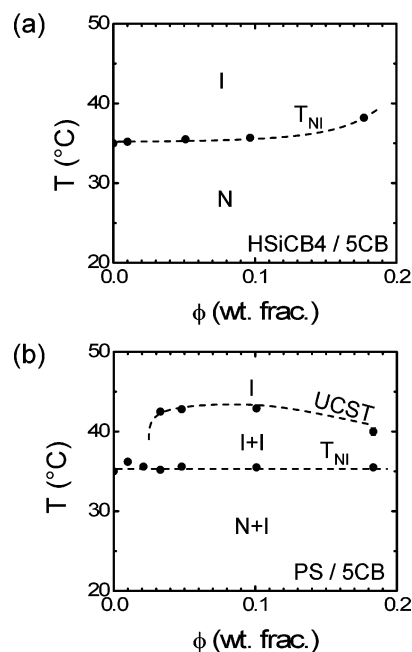


Figure 2. Partial binary phase diagrams of (a) HSiCB4 homopolymer in 5CB and (b) polystyrene homopolymer with 5CB. Dashed lines are drawn to guide the eye toward plausible phase boundaries.

solutions' gel-like nature preserves the alignment state after cessation of shear.

Results

Ternary Phase Behavior of PS, HSiCB4, and 5CB. The binary and ternary phase behavior of the coil and SGLCP homopolymers in the LC solvent provide the context for interpreting the behavior of the block copolymers. Binary solutions of HSiCB4 with 5CB were observed to be single phase both above and below T_{NI} , as previously reported^{20,22} (Figure 2a). Binary solutions of PS with nematic 5CB ($T < T_{\text{NI}}$) are phase-separated: a nematic phase coexists with an isotropic phase. The nematic always exhibits the same T_{NI} as pure 5CB, indicating that it has negligible PS dissolved in it. Thus, essentially all the PS is in the isotropic phase. At low PS concentration ($c \leq 2$ wt %) the transition to the isotropic phase produces a homogeneous single phase. At greater PS concentrations, there is a small biphasic window in the isotropic phase (Figure 2b), and the solutions become single phase above an upper critical solution temperature (UCST) that is within 7.4 $^{\circ}\text{C}$ of T_{NI} . This result is consistent with previously established phase diagrams of PS with 5CB,^{23,24} which found the two to be miscible above 40 $^{\circ}\text{C}$, provided the concentration of PS is less than 50 wt %.

Below T_{NI} , Hori et al.²⁴ also found the nematic phase to be pure 5CB. They report the composition of the isotropic phase to be between ~ 40 and 55 wt % PS, well below the threshold of 70–75 wt % PS required for the PS-rich phase to be glassy. We can, therefore, be confident that the observed phase behavior is near equilibrium.

Below T_{NI} , ternary mixtures of PS, HSiCB4, and nematic 5CB also separate into coexisting nematic and isotropic phases at all compositions tested. The measured isotropization points in ternary mixtures (i.e., transition from N + I to I + I biphasic or N + I to I) were found to be greater than or equal to T_{NI} of pure 5CB (35 $^{\circ}\text{C}$), indicating that the nematic phase contains little or no isotropic diluent. Dissolution of HSiCB4 can explain the observed increase in T_{NI} . Although the addition of HSiCB4 may modify the partitioning of 5CB between the two phases,

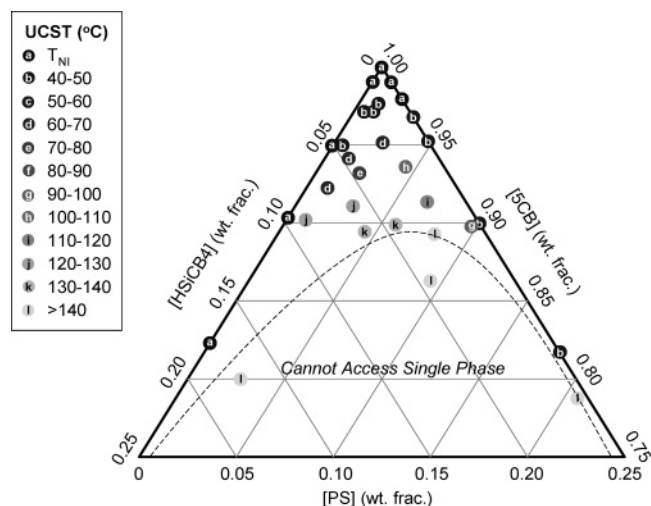


Figure 3. Partial ternary phase diagram of PS (44 kg/mol), HSiCB4, and isotropic 5CB determined from optical microscopy. The shading and letter of each point expresses the upper critical solution temperature (UCST) at which a single-phase solution is obtained. A UCST equal to T_{NI} means the solution became single-phase immediately upon transitioning to the isotropic phase. A UCST > 140 °C means a single phase was inaccessible because of thermal degradation. The dashed line is drawn to guide the eye to the region where a single-phase solution cannot be reached.

we expect the changes are small enough (change in PS concentration of less than 20 wt %) that the PS-rich phase does not become glassy, ensuring that our observations are, again, near equilibrium.

In isotropic 5CB, wide miscibility gaps were observed; i.e., the UCST is much greater than T_{NI} . The UCST of ternary mixtures of PS, HSiCB4, and isotropic 5CB was found to be highly sensitive to the concentrations of the two polymers (Figure 3). For example, holding the concentration of HSiCB4 fixed at 4.5 wt %, the addition of 0.5 wt % PS opens up a 14 °C miscibility gap (UCST = 49 °C), which expands to 97 °C (UCST = 132 °C) as the concentration of PS increased to 6 wt %. When the overall concentration of polymer, PS and HSiCB4 combined, exceeds ~10 wt %, the UCST cannot be reached before the sample thermally degrades, representing an effective solubility limit. This steep increase in UCST with increasing polymer concentration is striking because the UCST of the individual polymer solutions is never more than 7.4 °C above T_{NI} .

Rheometry. Rheometry was used to probe the temperature-dependent mechanical properties of diblock solutions. The solvent's temperature dependence is removed from the data by normalizing by the shear viscosity of 5CB (η_{5CB}) at the same temperature. In a 10 wt % solution of ABSiCB4 in nematic 5CB (Figure 4) the magnitude of the complex viscosity, $|\eta^*|$, varies inversely with frequency, ω , akin to an elastic solid ($G'' \ll G' \approx \text{constant}$). In contrast, in the isotropic phase at $T \geq 50$ °C, $|\eta^*|$ is nearly independent of ω , similar to a viscous liquid ($G' \ll G'' \approx \eta\omega$), and shifted data collapse onto a single curve. At temperatures between T_{NI} and 50 °C, the viscous response is intermediate between an elastic solid and viscous liquid. Similar behavior was observed in 5 and 20 wt % solutions. The temperature range for viscoelastic behavior increased with polymer concentration: viscous liquid response was first observed at 40 °C for the 5 wt % solution and 80 °C for the 20 wt % solution.

Small-Angle Neutron Scattering (SANS). SANS experiments give insight into the temperature-dependent structure of diblock copolymers in solution. In nematic solutions, a strong

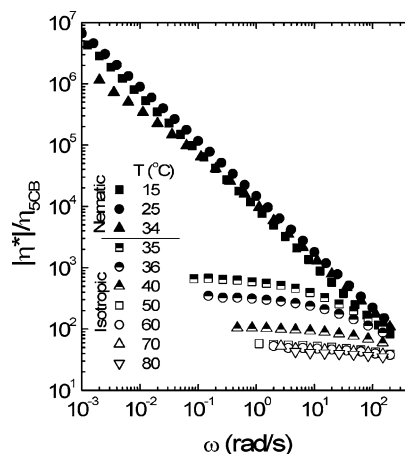


Figure 4. Frequency (ω)-dependent complex viscosity ($|\eta^*|$) as a function of temperature for 10 wt % ABSiCB4 in 5CB. Data are divided by the shear viscosity of 5CB (η_{5CB}) to remove the temperature dependence of the solvent's viscosity. In the nematic phase (filled symbols), PS blocks strongly associate and the material behaves as an elastic solid. Weak PS association is observed in a narrow temperature window (half-filled symbols) in the isotropic phase, and viscoelastic behavior is observed. At high temperature, the polymer acts as free chains in solution (unfilled symbols) and the material responds as a viscous liquid.

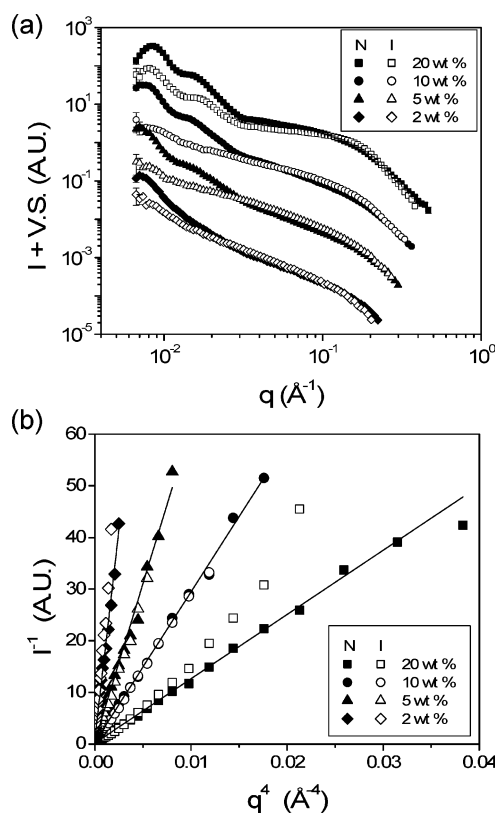


Figure 5. (a) Azimuthally averaged small-angle neutron scattering (SANS) patterns from solutions of ABSiCB4 diblock copolymer in perdeuterated 5CB at concentrations of 2, 5, 10, and 20 wt % and temperatures in the nematic (25 °C, closed symbols) and isotropic (37 °C, open symbols) phases. Data sets for concentrations less than 20 wt % are successively shifted down 1 order of magnitude for clarity. When not visible, error bars are smaller than the symbols. (b) Plotting I^{-1} vs q^4 at high values of q reveals the Porod law scaling characteristic of micellar structures.

peak is observed between approximately 0.0070 and 0.0085 \AA^{-1} for all concentrations (Figure 5a). The peak position varies weakly, if at all, with concentration. Peaks at higher q (between 0.0110 and 0.0350 \AA^{-1}) are apparent in the nematic phase for

concentrations of 5, 10, and 20 wt %. All isotropic samples have diminished intensity relative to the nematic data in the low- q (less than $\sim 0.035 \text{ \AA}^{-1}$) region (Figure 5a). On the other hand, at intermediate values of q (between ~ 0.035 and 0.11 \AA^{-1}) the intensity of the isotropic data is comparable to the nematic data. In the highest decade of q the scattered intensity of nematic solutions scales very nearly with q^{-4} for all concentrations (Figure 5b). Isotropic solutions scale with q^{-4} at high q only at concentrations of 2, 5, and 10 wt % polymer; the 20 wt % solution shows negative deviation from this scaling.

Discussion

Thermodynamics of Ternary Homopolymer Solutions.

Binary and ternary mixtures of HSiCB4 and PS dissolved in 5CB show that nematic 5CB is a strongly selective solvent. As previously reported by Hori et al.,²⁴ PS is insoluble in nematic 5CB because of the entropic penalty associated with dissolving a random coil polymer (e.g., PS) in an ordered solvent.^{18,19,24} On the other hand, HSiCB4 is soluble in nematic 5CB at all concentrations tested to date (up to 20 wt %).^{20,22} The chemically similar side groups of the liquid crystalline polymer midblock facilitate miscibility with the nematic solvent.

The observation of large miscibility gaps in ternary mixtures of PS, HSiCB4, and 5CB was surprising because single-phase solutions are easily achieved in binary mixtures of 5CB with either polymer alone. It is tempting to attribute phase separation to unfavorable interactions between the polymers themselves (a large contribution of χ_{AB}); however, this explanation is unsatisfactory in dilute solutions where polymer–polymer interactions are effectively screened by solvent. On the basis of the radius of gyration (R_g) of HSiCB4 determined using SANS ($\sim 100 \text{ \AA}$ at 25°C), the overlap concentration (c^*) is predicted to be $\sim 17 \text{ wt \%}$ at 25°C and is relatively insensitive to temperature. The overlap concentration of PS is calculated to be $\sim 7 \text{ wt \%}$ at 35°C in cyclohexane²⁵ ($R_g \sim 60 \text{ \AA}$), which represents a lower bound since 5CB is not as good a solvent for PS as cyclohexane. Although the radius of gyration of HSiCB4 is larger than that of PS, it has a much higher molecular weight ($\sim 470 \text{ kg/mol}$) than PS ($\sim 44 \text{ kg/mol}$) and, consequently, a higher c^* . The majority of our phase diagram is, therefore, well within a regime where the free energy contribution of interpolymer interaction (χ_{AB}) should be negligible.

The observed phase behavior at $c < c^*$ must then be attributed to polymer–solvent interactions and can be explained by the Patterson¹⁵–Prausnitz¹¹ treatment of the Scott¹³–Tompa¹⁴ theory for ternary polymer–polymer solutions. Patterson and Prausnitz found that any differential preference of the solvent for one polymer over the other ($\chi_{AS} \neq \chi_{BS}$), even if that preference is small, can induce phase separation. Furthermore, the effect is exacerbated when the molecular weight difference between the polymers is large. Therefore, phase separation at low concentrations of PS and HSiCB4 can be attributed to the asymmetric solvent effect: the chemical structure of the two polymers is sufficiently different to cause an appreciable difference in polymer–solvent interactions between the two, and the molecular weight ratio of PS to HSiCB4 is approximately 1:10.

Structural Transitions Caused by Change in Solvent Quality. The rheology of diblock copolymer solutions is correlated to the self-assembled structure of the polymer.^{26,27} In nematic solvent, elastic gels result from strong interactions between dense-core micelles. The abrupt decrease in elastic character at the isotropization point accords with the ternary phase behavior of homopolymers: upon isotropization, the

penetration of solvent into the micelles increases, causing a transition to highly swollen, soft micelles. The change from viscoelastic to viscous liquid behavior as temperature is increased within the isotropic phase accords with the dissolution of micellar structures to yield a solution of free polymer chains. The temperature dependence of the solution viscosity for $T \geq 50^\circ\text{C}$ is fully accounted for by the temperature dependence of the solvent's viscosity, indicating that PS block associations are negligible in this temperature range.

Attempts to quantitatively fit the SANS data to models are ongoing. Here we focus on qualitative conclusions that may be drawn from the data. The scattered intensity from a solution of block copolymer micelles is written as²⁸

$$I(q) = K[F_{\text{mic}}(q) + A_{\text{mic}}^2(q)(S(q) - 1)] \quad (1)$$

where $F_{\text{mic}}(q)$ is the form factor describing intraparticle correlations for block copolymer micelles, $S(q)$ is the structure factor describing interparticle correlations, $A_{\text{mic}}(q)$ is the form factor amplitude of the radial scattering length distribution, and K is a constant. At dilute concentration (and at very large values of q) the micellar fluid structure is random (particle positions are uncorrelated), so the structure factor equals unity ($S(q) = 1$). Therefore, $F_{\text{mic}}(q)$ can be determined in dilute solutions.

Peaks in the scattering data from nematic solutions have positions that are relatively insensitive to concentration (Figure 5a) and are, therefore, unlikely to be associated purely with the structure factor; the position of the first peak shifts only 20% to greater q as concentration is increased 10-fold. Therefore, the scattering from the most dilute solution (2 wt %) may be taken as a close approximation of the form factor, $F_{\text{mic}}(q)$. As polymer concentration is increased, additional contributions of $S(q)$ further the amplitude of oscillations in intensity. Using the experimentally determined $F_{\text{mic}}(q)$, the structure factor for the 5 and 10 wt % solutions can be estimated as

$$S(q) \approx \frac{I(q)}{cF_{\text{mic}}(q)} \quad (2)$$

where c is the ratio of polymer concentrations (e.g., $c = 5/2$ for 5 wt % solution). Indeed, this yields a plausible envelope for the structure factor of $S(q) = 1 \pm 0.4$. Because structure factor variations are small, there is little shift in peak position with concentration. The main effect of the structure factor is to increase the magnitude of low- q oscillations.

Structural transitions observed by rheometry are corroborated by SANS. The decrease in low- q intensity that takes place with isotropization is evidence that LC solvent penetrates the micelle cores. The scattering at low q is dominated by the corona contribution to $F_{\text{mic}}(q)$,²⁹ which is determined by the radial density profile of polymer chains in the corona. A decrease in intensity implies a decrease in polymer concentration in the corona, but the relatively constant intensity at intermediate q , where single-chain scattering is dominant, indicates that the radius of gyration of the corona chains (and hence the swelling of individual corona chains) is not substantially altered by the transition. Rather, the swelling of the core yields a larger area of core surface per corona chain, and the SGLCP blocks are less crowded at the core–corona interface. This is consistent with the decrease in aggregation number and decrease in the local density of corona chains at the core surface observed in conventional block copolymer micelles when cores become swollen with solvent near the critical micelle temperature.¹⁶

The peaks characteristic of $F_{\text{mic}}(q)$ in the low- q regime of nematic solutions virtually disappear upon isotropization, mak-

ing it difficult to discern whether neutron scattering is from micelles or from free chains in solution. However, data in the high- q regime give evidence that micelles exist in both nematic and isotropic samples. The terminal scaling of intensity with q for a system having a sharp interface between regions of different scattering length density (e.g., between a micelle's core and corona) is described by the Porod law:³⁰

$$I(q) = \frac{b_v^2 2\pi S_T}{q^4} + I_b \quad (3)$$

where b_v^2 is the contrast in scattering length density across the interface, S_T is the total area of the interface, and I_b is the incoherent background scattering, assumed to be q -independent. Thus, at large q the background-subtracted intensity ($I(q) - I_b$) multiplied by q^4 exhibits a plateau with magnitude (Porod constant) proportional to the total surface area and to the neutron scattering contrast at the interface. Nematic samples exhibit the expected Porod scaling at all concentrations. Porod scaling is also observed in isotropic samples with concentration ≤ 10 wt % and is evidence that micellar structures still exist. Remarkably, the Porod constant for these solutions changes very little upon isotropization. The increase in size that occurs when 5CB swells the micelle core is partially offset by the decrease in contrast (eq 3), and when combined with uncertainties inherent to the background subtraction, the change in Porod constant is barely observable. Although the highest- q data for the isotropic 20 wt % solution deviate from Porod scaling, micellization is clearly evidenced by prominent peaks (Figure 5a). The deviation from Porod scaling in this sample is likely due to the presence of a diffuse interface.

Driving Force for Self-Assembly of Diblock Copolymer.

Ternary mixtures of HSiCB4 and PS in 5CB show that the selectivity of 5CB changes discontinuously at T_{NI} : in the nematic phase 5CB is strongly selective toward HSiCB4, and in the isotropic phase it is less selective. The change in selectivity translates to changes in the self-assembled structures of the analogous diblock copolymer, ABSiCB4, in 5CB. The self-assembly of the block copolymer reflects the same thermodynamic driving forces that cause phase separation in homopolymer solutions.

Below the isotropization point, both SANS and rheometry give clear evidence of PS associations at all concentrations tested. The self-assembly of the diblock copolymer to form micelles is simply driven by the strong selectivity of the LC solvent in the nematic phase. Upon isotropization, the solvent selectivity decreases and the micelles are observed to undergo significant structural changes as they swell with isotropic solvent. In dilute (≤ 10 wt %) solutions, the Patterson–Prausnitz asymmetric solvent effect that causes macrophase separation in ternary homopolymer solutions also drives the association of PS end blocks. When the concentrated regime is approached (20 wt %) the contribution of χ_{AB} becomes increasingly important, and as is typically the case in ternary polymer solutions,¹² polymer–polymer interactions are probably the primary driving force behind the observed PS block association. Above a critical temperature, the micelles dissolve and a simple polymer solution is obtained.

Conclusion

The dominant thermodynamic interaction driving self-assembly of a block copolymer in a LC solvent can be modulated with small changes in temperature and concentration. Unfavorable 5CB–PS interactions dominate in the nematic phase; in

the isotropic phase unfavorable PS–SGLCP interactions dominate at high concentrations ($c > c^*$), and the asymmetric solvent effect (the preference of 5CB for SGLCP) dominates at lower concentrations.

In the context of the literature on block copolymers in isotropic solvents, the results presented here imply that new juxtapositions of ordered phases can be introduced into their phase diagrams. The progression of ordered phases that would conventionally be observed in two separate solvents of different quality (strongly selective^{5,7,9} vs slightly selective^{3,6,8}) can now be combined into the single phase diagram of a given block copolymer in a single LC solvent. Small temperature changes could switch the system between the two regimes of ordered phases. The present system switches from a disordered micelle phase that is relatively rigid and has a low volume fraction of the PS-rich domains to a different disordered micelle phase that is much softer and has a substantial volume fraction of the PS-rich domains. This suggests that for other relative block lengths and concentrations the system could jump between ordered phases (e.g., fcc and bcc) very abruptly with temperature.

Acknowledgment. This work benefited from use of the shared facilities supported by the MRSEC Program of the National Science Foundation under Award DMR-0080065. The authors also acknowledge financial support from the AFOSR LC-MURI (f4962-97-1-0014). We thank Ed Lang (Argonne National Laboratory, Intense Pulsed Neutron Source) for assistance with SANS experiments and Rafael Verduzco for helpful discussions. A National Defense Science and Engineering Graduate Fellowship awarded to N.R.S. is greatly appreciated.

References and Notes

- (1) Park, C.; Yoon, J.; Thomas, E. L. *Polymer* **2003**, *44*, 6725.
- (2) Hamley, I. W. *The Physics of Block Copolymers*; Oxford University Press: Oxford, 1998.
- (3) Hamley, I. W.; Fairclough, J. P. A.; Ryan, A. J.; Ryu, C. Y.; Lodge, T. P.; Gleeson, A. J.; Pedersen, J. S. *Macromolecules* **1998**, *31*, 1188.
- (4) Hanley, K. J.; Lodge, T. P.; Huang, C.-I. *Macromolecules* **2000**, *33*, 5918.
- (5) Lai, C.; Russel, W. B.; Register, R. A. *Macromolecules* **2002**, *35*, 841.
- (6) Lodge, T. P.; Hanley, K. J.; Pudil, B.; Alahapperuma, V. *Macromolecules* **2003**, *36*, 816.
- (7) Lodge, T. P.; Pudil, B.; Hanley, K. J. *Macromolecules* **2002**, *35*, 4707.
- (8) Lodge, T. P.; Xu, X.; Ryu, C. Y.; Hamley, I. W.; Fairclough, J. P. A.; Ryan, A. J.; Pedersen, J. S. *Macromolecules* **1996**, *29*, 5955.
- (9) McConnell, G. A.; Gast, A. P. *Macromolecules* **1997**, *30*, 435.
- (10) Lodge, T. P.; Blazey, M. A.; Liu, Z. *Macromol. Chem. Phys.* **1997**, *198*, 983.
- (11) Hsu, C. C.; Prausnitz, J. M. *Macromolecules* **1974**, *7*, 320.
- (12) Olabisi, O.; Robeson, L. M.; Shaw, M. T. *Polymer–Polymer Miscibility*; Academic Press: San Diego, 1979; pp 157–166.
- (13) Scott, R. L. *J. Chem. Phys.* **1949**, *17*, 279.
- (14) Tompa, H. *Trans. Faraday Soc.* **1949**, *45*, 1142.
- (15) Zeman, L.; Patterson, D. *Macromolecules* **1972**, *5*, 513.
- (16) Bang, J.; Viswanathan, K.; Lodge, T. P.; Park, M. J.; Char, K. *J. Chem. Phys.* **2004**, *121*, 11489.
- (17) Lodge, T. P.; Bang, J.; Park, M. J.; Char, K. *Phys. Rev. Lett.* **2004**, *92*, 145501.
- (18) Benmouna, F.; Daoudi, A.; Roussel, F.; Buisine, J.-M.; Coqueret, X.; Maschke, U. *J. Polym. Sci., Part B: Polym. Phys.* **1999**, *37*, 1841.
- (19) Gogibus, N.; Maschke, U.; Benmouna, F.; Ewen, B.; Coqueret, X.; Benmouna, M. *J. Polym. Sci., Part B: Polym. Phys.* **2001**, *39*, 581.
- (20) Kempe, M. D.; Verduzco, R.; Scruggs, N. R.; Kornfield, J. A. *Soft Matter* **2006**, *2*, 422.
- (21) Wu, S. T.; Wang, Q. H.; Kempe, M. D.; Kornfield, J. A. *J. Appl. Phys.* **2002**, *92*, 7146.

- (22) Kempe, M. D.; Scruggs, N. R.; Verduzco, R.; Lal, J.; Kornfield, J. A. *Nat. Mater.* **2004**, *3*, 177.
- (23) Hakemi, H. *Polymer* **1999**, *40*, 4099.
- (24) Hori, H.; Urakawa, O.; Adachi, K. *Macromolecules* **2004**, *37*, 1583.
- (25) Brandup, J.; Immergut, E. H.; Grulke, E. A. *Polymer Handbook*, 4th ed.; Wiley: New York, 1999.
- (26) Higgins, J. S.; Blake, S.; Tomlins, P. E.; Ross-Murphy, S. B.; Staples, E.; Penfold, J.; Dawkins, J. V. *Polymer* **1988**, *29*, 1968.
- (27) Prud'homme, R. K.; Wu, G.; Schneider, D. K. *Langmuir* **1996**, *12*, 4651.
- (28) Pedersen, J. S. *J. Chem. Phys.* **2001**, *114*, 2839.
- (29) Scruggs, N. R.; Verduzco, R.; Lal, J.; Kornfield, J. A. Manuscript in preparation.
- (30) Higgins, J. S.; Benoit, H. C. *Polymers and Neutron Scattering*; Oxford University Press: New York, 1996; pp 165–184.

MA052414O